Aluminum substitution for Vanadium in the $Na_3V_2(PO_4)_2F_3$ and $Na_3V_2(PO_4)_2FO_2$ type materials

Jacob Olchowka [a,d,e], Long H. B. Nguyen [a,b,d], Thibault Broux [a,b,d,e], Paula Sanz Camacho [a,d], Emmanuel Petit [a,d,e], François Fauth [c], Dany Carlier [a,d,e], Christian Masquelier [b,d,e] and Laurence Croguennec [a,d,e,*]

[a] CNRS, Univ. Bordeaux, Bordeaux INP, ICMCB UMR 5026, F-33600, Pessac, France.

[b] Laboratoire de Réactivité et de Chimie des Solides, CNRS-UMR# 7314, Université de Picardie Jules Verne, F-80039 Amiens Cedex 1, France.

[c] CELLS-ALBA synchrotron, E-08290 Cerdanyola del Vallès, Barcelona, Spain.

[d] RS2E, Réseau Français sur le Stockage Electrochimique de l'Energie, FR CNRS 3459, F-80039 Amiens Cedex 1, France.

[e] ALISTORE-ERI European Research Institute, FR CNRS 3104, Amiens, F-80039 Cedex 1, France.

Supporting Information

Experimental part

Laboratory X-ray powder diffraction (XRPD) was carried out using a PANalytical Empyrean diffractometer in θ-θ configuration and equipped with a Cu $K_{\alpha 1,2}$ X-ray source. The acquisition was performed in the 2θ range of 8° – 80 with a step size of 0.0167°. The full pattern matching for the $Na_3V_{2-z}Al_z(PO_4)_2F_{1+z}O_{2-z}$ ($0 \leq z \leq 2$) materials was performed using Fullprof software.

High-resolution synchrotron powder X-ray diffraction (SXRPD) was performed at the MSPD beamline at ALBA (Barcelona, Spain). The powders were packed in a 0.5 mm diameter capillary and mounted on a goniometer in Debye – Scherrer geometry. The data were recorded by using the MYTHEN detector at a wavelength of 0.6202 Å, in the 2θ angular range of 1° – 70° with a 0.006° step. Diffraction data analysis and Rietveld refinement were performed by utilizing FullProf Suite. The 3D crystal structure of the materials were visualized by using VESTA software.

The chemical analysis of the Na, V, Al and P contents was performed by inductively coupled plasma-optical emission spectroscopy (ICP-OES) using a Varian Model 720-ES spectrometer, after a dissolution of the powders into a concentrated hydrochloric acid (HCl) solution. Typically 20mg of powder are put into 5mL of HCl solution under stirring to be dissolved. Then the volume was adjusted to 100mL with distilled water. A test was performed by replacing our material by commercial $AlPO_4$ in the same experimental conditions. After several hours of stirring, $AlPO_4$ was dispersed in the solution but not dissolved which can explain the apparent cationic ratio determined for *NVPFO-$Al_{0.5}$-basic*

* Corresponding author (Laurence.Croguennec@icmcb.cnrs.fr)

($Na_3V^{4+}_{1.5}Al_{0.5}(PO_4)_2F_{1.5}O_{1.5}$) material. It is important to remind that the water-soluble impurities (such as $Na_5P_5O_{10}$ and Na_3VF_6) were removed during the washing step.

Fourier transformed infrared (FT-IR) spectra were recorded by using a Bruker Equinox 55 spectrometer in the wavenumber range of 400 - 4000 cm^{-1} (mid-IR) with a resolution of 4 cm^{-1}. The samples were finely ground in a mortar with dried KBr in an approximate ratio of 3: 50 (by wt.%).

^{31}P ss-NMR spectra were acquired on a Bruker Avance III 100 MHz spectrometer, equipped with a 2.4 T widebore magnet (operating at Larmor frequency of 40.6 MHz for ^{31}P) by using a standard Bruker 2.5 mm MAS probe at 30 kHz magic angle spinning rate. Chemical shifts are referenced relative to an aqueous H_3PO_4 85% (Sigma-Aldrich) solution at 0 ppm. In each case, a Hahn echo sequence was used with a $\pi/2$ pulse of 1.1 µs and a recycle delay of 0.2 s.

The electrochemical properties of the materials were tested in CR2032-type coin cells. The positive electrodes were prepared by mixing homogeneously a mixture containing 80 wt.% active material, 10 wt.% Carbon black, and 10 wt.% polytetrafluoroethylene (PTFE). The as-obtained mixture was pressed under 10 tons to form films with a thickness of ~ 150 µm and then dried overnight at 80°C under vacuum. A homemade electrolyte containing 1M solution of $NaPF_6$ (Strem Chemical; 99%) in ethylene carbonate and dimethyl carbonate (EC: DMC = 1: 1) with 2 wt.% of fluoroethylene carbonate (FEC) was used in all the electrochemical tests. The assembled cells were cycled in galvanostatic mode, at a C/10 cycling rate between 2.8 and 4.5 V vs. Na^+/Na. The rate C/10 corresponds to the exchange of 1 Na^+ in 10 hours. For *NVPFO-$Al_{0.5}$-basic* material, only 88% of the total material mass was taking as active mass, the 12 wt% of $AlPO_4$ determined by Rietveld refinement was not taken into account.

* Corresponding author (Laurence.Croguennec@icmcb.cnrs.fr)

Figure S1. *Rietveld refinement of synchrotron powder X-ray diffraction data recorded at λ = 0.6202 Å for: a) NVPF-$Al_{0.5}$-acidic refined in the Amam space group and b) NVPFO-$Al_{0.5}$-basic refined in the $P4_2/mnm$ space group. The secondary phase (bottom grey tick lines) corresponds to $AlPO_4$ and its concentration is refined to ~12.1 wt.%.*

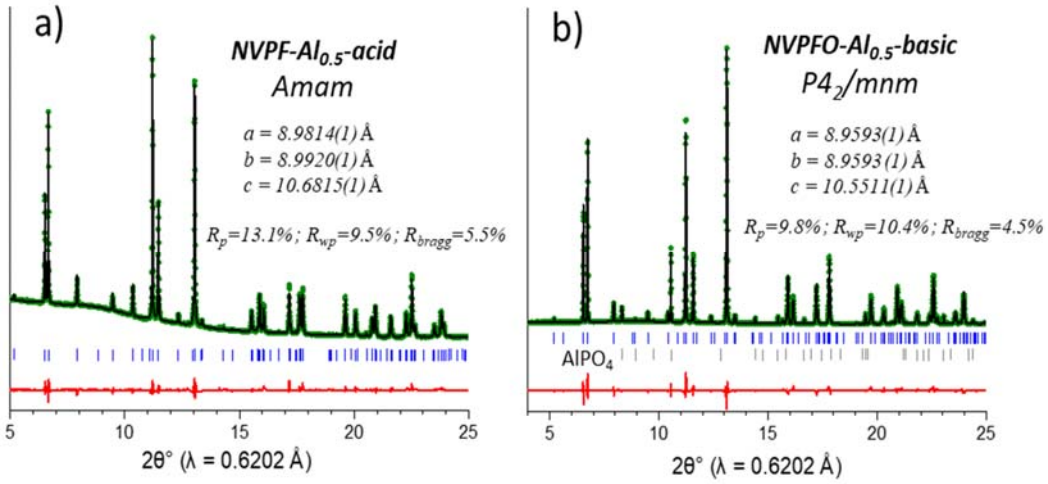

* Corresponding author (Laurence.Croguennec@icmcb.cnrs.fr)

Structural determination of $Na_3V_{1.5}Al_{0.5}(PO_4)_2F_3$ (NVPF-$Al_{0.5}$-acidic)

Figure S2. Comparison of the structural description of $Na_3V_{1.5}Al_{0.5}(PO_4)_2F_3$ in the Amam and $P4_2/mnm$ space groups.

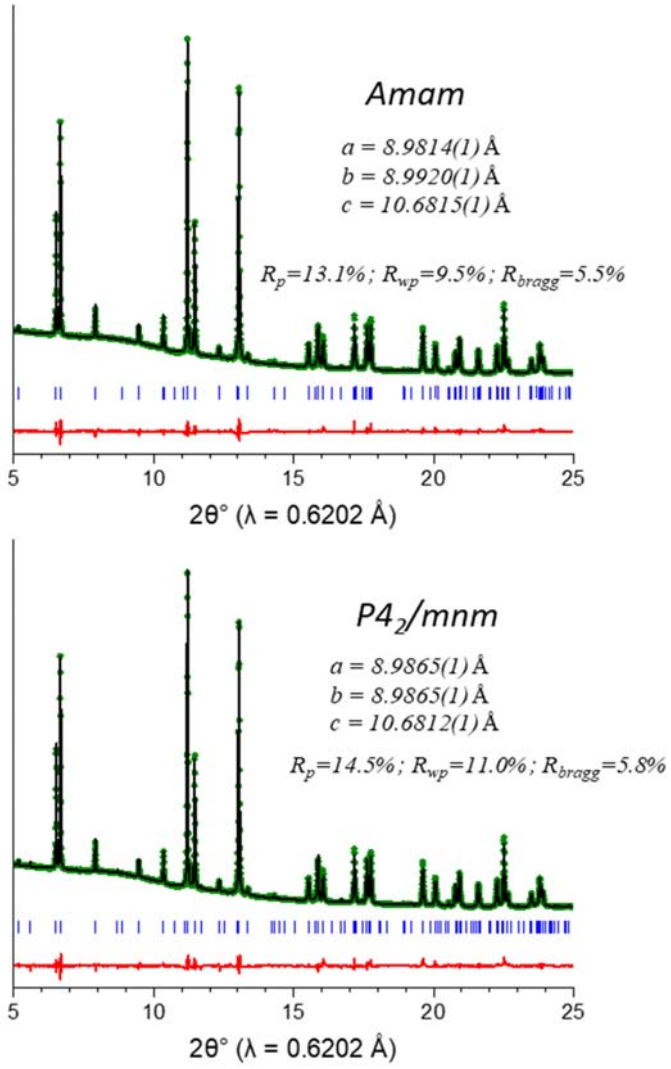

Comparison of the **Rietveld refinements** of synchrotron powder X-ray diffraction data of $Na_3V_{1.5}Al_{0.5}(PO_4)_2F_3$ recorded at λ = 0.6202 Å. Although the reliability factors are slightly better considering the Amam space group, the description of the structure in the *Amam* and *$P4_2/mnm$* space groups shows a rather good minimization of the difference (*Iobs.* - *Icalc.*) for both cases.

* Corresponding author (Laurence.Croguennec@icmcb.cnrs.fr)

Table S1. A comparison of the interatomic distances in $Na_3V^{3+}_{1.5}Al_{0.5}(PO_4)_2F_3$ obtained from Rietveld refinement by considering the $P4_2/mnm$ and Amam space groups.

$Na_3V_{1.5}Al_{0.5}(PO_4)_2F_3$			
Amam		*$P4_2/mnm$*	
R_{Bragg} = 5.5% R_p = 13.1% R_{wp} = 9.5%		R_{Bragg} = 5.8% R_p = 14.5% R_{wp} = 11.0%	
	Interatomic distances (Å)		**Interatomic distances (Å)**
P(1)─O(1)	1.512(6) x 2	**P(1)─O(1)**	1.531(5) x **4**
P(1)─O(2)	1.569(6) x 2	**P(2)─O(3)**	1.598(10) x **2**
		P(2)─O(2)	1.509(8) x **2**
V/Al(1) ─O(1)	1.956(6) x 2	**V(1) ─O(1)**	1.988(8) x **2**
V/Al(1) ─O(2)	1.967(7) x 2	**V(1) ─O(2)**	1.923(7)
		V(1) ─O(3)	1.946(7)
V(1) ─F(1)	1.956(1)	**V(1) ─F(1)**	1.958(2)
V(1) ─F(2)	1.928(2)	**V(1) ─F(2)**	1.945(2)
Na(1)-Na(1)	4.521(2)	**Na(1)-Na(1)**	3.023(8)
Na(1)-Na(2)	3.234(1)	**Na(1)-Na(2)**	3.106(7)
Na(1)-Na(3)	2.692(10)	**Na(2)-Na(2)**	1.418(8)

* Corresponding author (Laurence.Croguennec@icmcb.cnrs.fr)

Figure S3. Fourier difference maps of $Na_3V_{1.5}Al_{0.5}(PO_4)_2F_3$ in the Amam and $P4_2/mnm$ space groups.

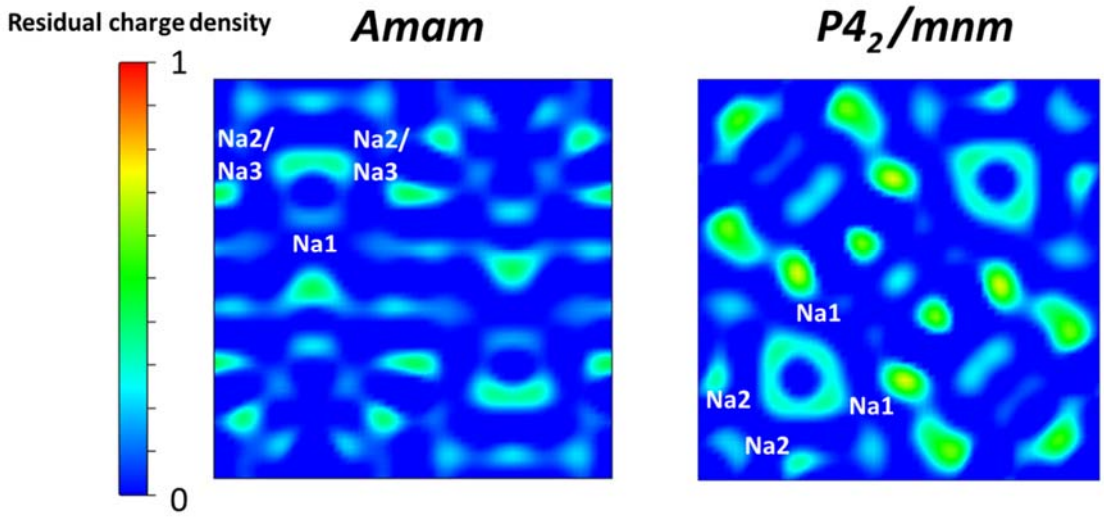

The comparison of the interatomic distances in $Na_3V_{1.5}Al_{0.5}(PO_4)_2F_3$ obtained from Rietveld refinement reveals that the vanadium/aluminum octahedral environments and the phosphorus (P2) tetrahedral environment are more distorted in the *P*4_2*/mnm* space group than in the *Amam* one. The distance Na(2)-Na(2) is too short in the *P*4_2*/mnm* space group (1.418 Å with an occupancy of 0.7 for the Na(2) site) whereas it is suitable in the *Amam* one. Finally, the corresponding Fourier difference maps show higher residues for the structural model described in the tetragonal symmetry. All these information support the choice of the orthorhombic model to describe the $\mathbf{Na_3V^{3+}_{1.5}Al_{0.5}(PO_4)_2F_3}$ phase.

* Corresponding author (Laurence.Croguennec@icmcb.cnrs.fr)

Table S2: Structural parameters determined for $Na_3V^{3+}_{1.5}Al_{0.5}(PO_4)_2F_3$ by the Rietveld refinement of the synchrotron powder diffraction data in the Amam space group.

$Na_3V_{1.5}Al_{0.5}(PO_4)_2F_3$ (NVPF-$Al_{0.5}$-acid)

S.G. Amam *Z* = 4		*a* = 8.9814(1) Å *b* = 8.9920(1) Å *c* = 10.6815(1) Å *V* = 862.65(1) Å^3				R_{Bragg} = 5.5% R_p = 13.1% R_{wp} = 9.5%
Atoms	**Wyckoff positions**	***x***	***y***	***z***	**Occupancy**	**B_{iso}**
V (1)	8g	1/4	0.2481(4)	0.1831(1)	0.75	0.79(2)
Al (1)	8g	1/4	0.2481(4)	0.1831(1)	0.25	0.79(2)
P (1)	8e	0	1/2	0.2458(5)	1	1.11(3)
O (1)	16h	0.1006(6)	0.4050(7)	0.1654(5)	1	0.9(1)
O (2)	16h	0.0933(5)	0.0976(7)	0.1609(4)	1	1.3(1)
F (1)	4c	1/4	0.2455(12)	0	1	0.73(8)
F(2)	8g	1/4	0.2548(11)	0.3635(2)	1	1.59(6)
Na (1)	4c	1/4	0.0289(11)	1/2	0.899(13)	3.5(4)
Na (2)	8f	0.5696(7)	0.1515(11)	0	0.530(11)	3.5(3)
Na (3)	8f	-0.0292(9)	0.2686(9)	0	0.548(11)	1.7(3)

* Corresponding author (Laurence.Croguennec@icmcb.cnrs.fr)

Table S3. Comparison of the space group, cell parameters and volume describing the structure of the different synthesized materials.

Composition	Space group	a (Å)	b (Å)	b/a	c (Å)	V/Z (Å^3)
$Na_3V^{3+}_2(PO_4)_2F_3$ [1]	*Amam*	9.0285(1)	9.0444(1)	1.002	10.7466(1)	219.46(1)
$Na_3V^{3+}_{1.9}Al_{0.1}(PO_4)_2F_3$ [2]	*Amam*	9.016(1)	9.032(1)	1.002	10.732(1)	218.5(1)
$Na_3V^{3+}_{1.8}Al_{0.2}(PO_4)_2F_3$ [2]	*Amam*	9.002(3)	9.026(3)	1.003	10.716(3)	217.7(3)
$Na_3V^{3+}_{1.7}Al_{0.3}(PO_4)_2F_3$ [2]	*Amam*	8.990(1)	9.010(1)	1.002	10.704(1)	216.8(2)
$Na_3V^{3+}_{1.5}Al_{0.5}(PO_4)_2F_3$ (this work)	*Amam*	8.9814(1)	8.9920(1)	1.001	10.6815(1)	215.6(1)
$Na_3(V^{4+}O)_2(PO_4)_2F$ [3]	*P4$_2$/mnm*	9.0287(9)	9.0287(9)	1	10.6056(1)	216.13(1)
$Na_3V^{4+}_{1.75}Al_{0.25}(PO_4)_2F_{1.25}O_{1.75}$ (this work)	*P4$_2$/mnm*	8.992(1)	8.992(1)	1	10.591(1)	214.2(1)
$Na_3V^{4+}_{1.50}Al_{0.50}(PO_4)_2F_{1.50}O_{1.50}$ (this work)	*P4$_2$/mnm*	8.9593(1)	8.9593(1)	1	10.5511(1)	211.7(1)
$Na_3V^{4+}_{1.25}Al_{0.75}(PO_4)_2F_{1.75}O_{1.25}$ (this work)	*P4$_2$/mnm*	8.918(1)	8.918(1)	1	10.522(1)	209.2(1)
$Na_3V^{4+}_{0.75}Al_{1.25}(PO_4)_2F_{2.25}O_{0.75}$(this work)	*P4$_2$/mnm*	8.864(1)	8.864(1)	1	10.482(1)	206.5(2)
$Na_3V^{4+}_{0.50}Al_{1.50}(PO_4)_2F_{2.50}O_{0.50}$ (this work)	*P4$_2$/mnm*	8.826(1)	8.826(1)	1	10.441(1)	202.8(1)
$Na_3Al_2(PO_4)_2F_3$ (this work)	*P4$_2$/mbc*	12.385(1)	12.385(1)	1	10.394(1)	199.3(1)

* Corresponding author (Laurence.Croguennec@icmcb.cnrs.fr)

Figure S4: Powder XRD patterns collected for the different phases belonging to the solid solution $Na_3V^{4+}_{2-z}Al_z(PO_4)_2F_{1+z}O_{2-z}$. The different V : Al ratio listed on the left were determined by ICP-OES analyses. Except for $V_{1.25}Al_{0.75}$, the impurity is attributed to $AlPO_4$.

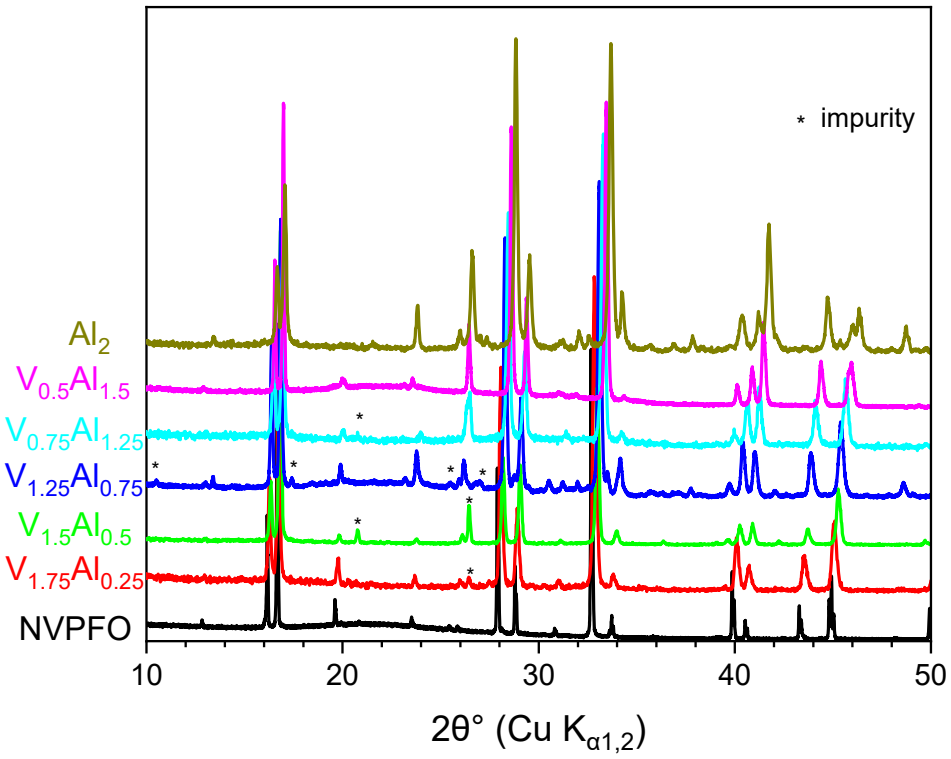

* Corresponding author (Laurence.Croguennec@icmcb.cnrs.fr)

Figure S5 a) Enlargement of the powder XRD patterns given in Figure S3 between 27.5 and 29.6 °(2θ). The different V : Al ratio listed on the left were determined by ICP-OES analyses b) Evolution of the cell parameter a and c according to the Al for V substitution.

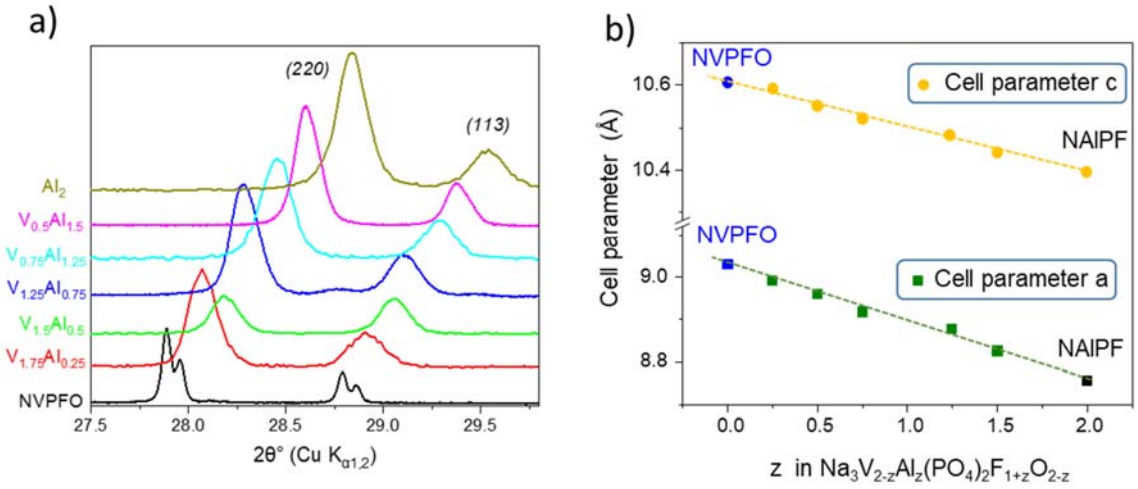

* Corresponding author (Laurence.Croguennec@icmcb.cnrs.fr)

Structural determination of $Na_3V_{1.5}Al_{0.5}(PO_4)_2F_{1.5}O_{1.5}$ (NVPFO-$Al_{0.5}$-basic)

Table S4: Structural parameters of $Na_3V^{4+}_{1.5}Al_{0.5}(PO_4)_2F_{1.5}O_{1.5}$ and obtained from the Rietveld refinement of the synchrotron powder diffraction data.

$Na_3V_{1.5}Al_{0.5}(PO_4)_2F_{1.5}O_{1.5}$ (NVPFO-$Al_{0.5}$-basic)						
S.G. $P4_2/mnm$ $Z = 4$		$a = 8.9593(1)$ Å $b = 8.9593(1)$ Å $c = 10.5511(1)$ Å $V = 846.93(1)$ Å^3				$R_{Bragg} = 4.5\%$ $R_p = 9.8\%$ $R_{wp} = 10.4\%$
Atoms	**Wyckoff positions**	***x***	***y***	***z***	**Occupancy**	**B_{iso}**
V (1)	8j	0.2495(3)	0.2495(3)	0.1964(1)	0.75	0.887(2)
Al (1)	8j	0.2495(3)	0.2495(3)	0.1964(1)	0.25	0.887(2)
P (1)	4d	0	1/2	1/4	1	0.8(2)
P (2)	4e	0	0	0.2566(5)	1	0.8(2)
O (1)	16k	0.0957(4)	0.4056(5)	0.1617(4)	1	0.9(2)
O (2)	8j	0.0965(5)	0.0965(5)	0.1677(8)	1	0.9(2)
O (3)	8j	0.4012(5)	0.4012(5)	0.1597(8)	1	0.9(2)
F (1)	4f	0.2468(6)	0.2468(6)	0	1	0.85(7)
F (2)/O (4)	8j	0.2481(6)	0.2481(6)	0.3531(1)	1	0.51(5)
Na (1)	8i	0.5174(5)	0.2395(6)	0	0.899(13)	2.0(1)
Na (2)	8i	0.8013(6)	0.0372(9)	0	0.530(11)	3.9(3)

* Corresponding author (Laurence.Croguennec@icmcb.cnrs.fr)

Table S5: Interatomic distances in $Na_3V^{4+}_{1.5}Al_{0.5}(PO_4)_2F_{1.5}O_{1.5}$ obtained from the Rietveld refinement of the SXRD data in the $P4_2/mnm$ space group.

$Na_3V_{1.5}Al_{0.5}(PO_4)_2F_{1.5}O_{1.5}$	
	Interatomic distances (Å)
P(1)─O(1)	1.523(4) x **4**
P(2)─O(3)	1.532(7) x **2**
P(2)─O(2)	1.541(7) x **2**
V(1) ─O(1)	1.997(5) x **2**
V(1) ─O(2)	1.962(8)
V(1) ─O(3)	1.961(5)
V(1) ─F(1)	2.072(8)
V(1) ─F(2)/O(4)	1.654(3)
Na(1)-Na(1)	3.080(7)
Na(1)-Na(2)	3.123 (8)
Na(2)-Na(2)	2.046 (10)

* Corresponding author (Laurence.Croguennec@icmcb.cnrs.fr)

Extended discussion of the possible origins of the greater polarization

When vanadium is partially substituted by aluminum, the hysteresis (polarization) is highly increased as can be seen in Figure 4. There are many factors that may lead to this hysteresis increase:

(i) V^{3+}/V^{4+} is a transition metal ion which possesses unpaired electron(s) and in $Na_3V_2(PO_4)_2F_3$ type materials, these vanadium ions reside in bi-octahedral units with the V^{n+}—F—V^{n+} bond linking the two neighboring vanadium ions. Thanks to this bridging fluorine, the vanadium's unpaired electron(s) can be transferred to its opposite site. This electron circulation, though rather weak, contributes to the electronic conductivity of the materials. When vanadium ions are substituted by Al^{3+}, no electron transfer will occur between the Al site and its neighboring V site belonging to the same pair. Furthermore, the presence of Al^{3+} in the structural framework will lead to an electron depletion in the conduction band close to the Fermi level. A combination of these two effects will decrease the materials' electronic conductivity. The higher the Al-content is, the lower the electronic conductivity which in turn induces a greater polarization. This is supported by the fact that the hysteresis observed for sodium cell with $Na_3V^{4+}_{1.5}Al_{0.5}(PO_4)_2F_{1.5}O_{1.5}$ at the positive electrode is smaller than that observed for $Na_3V^{4+}_{0.75}Al_{1.25}(PO_4)_2F_{2.25}O_{0.75}$ (Figure R1).

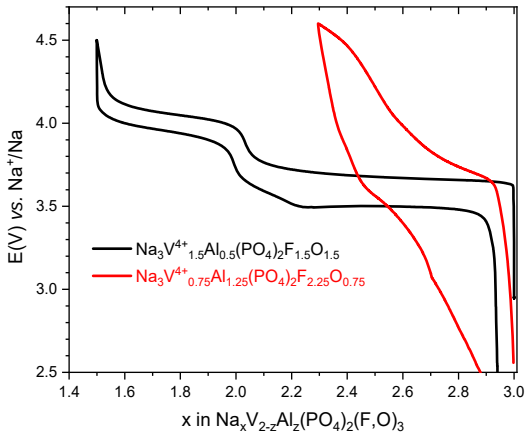

Figure S6: Comparison of the electrochemical profiles obtained for the sodium cells Na//$Na_3V^{4+}_{1.5}Al_{0.5}(PO_4)_2F_{1.5}O_{1.5}$ and Na//$Na_3V^{4+}_{0.75}Al_{1.25}(PO_4)_2F_{2.25}O_{0.75}$.

A higher hysteresis compared to NVPF was also observed by Bianchini et al. for $Na_3V_{1.7}Al_{0.3}(PO_4)_2F_3$ although it was not discussed in their paper (figure 5b in ref 16)

(ii) Al^{3+} has a smaller ionic radius than V^{3+} or V^{4+} (53.5 pm vs. 64 pm and 58 pm, respectively), and thus an Al^{3+} substitution will lead to a structural shrinkage (Figure 2b) which will in turn reduce the size of the Na^+ diffusion channels. In a recent theoretical work (*Chem. Mater.* 2016, 28, 5450-5460), Dacek *et al.* predicted that the size of the diffusion channels did not have a great impact on the Na^+ diffusion process in $Na_3V_2(PO_4)_2F_3$ type materials. Nevertheless, only a slight influence on the Na^+ diffusion process could induce a small increase in the material's hysteresis.

(iii) $Na_3V^{3+}_{1.5}Al_{0.5}(PO_4)_2F_3$ was reported to be pure (Figure 1a) and to contain the carbon residue from the acid citric decomposition during the calcination process. However, this carbon was obtained at 650°C only, as a higher calcination temperature was shown to be detrimental to the stability of the fluorinated phase. It contains mainly Csp^3, which is

* Corresponding author (Laurence.Croguennec@icmcb.cnrs.fr)

detrimental to the electronic conductivity and thus to electrochemical performance, especially at high rates. It can thus participate also to the increase of the hysteresis.

(iv) In the specific case of $Na_3V^{4+}_{1.5}Al_{0.5}(PO_4)_2F_{1.5}O_{1.5}$ (Figure 4a), $AlPO_4$ impurity was detected by XRD. As $AlPO_4$ is an insulator, it will lower the electronic conductivity of the material as compared to $Na_3V^{4+}_2(PO_4)_2FO_2$ which was obtained as pure phase.

* Corresponding author (Laurence.Croguennec@icmcb.cnrs.fr)

Figure S7. The electrochemical profiles of Na//$Na_3V_{1.5}Al_{0.5}(PO_4)_2F_3$ in the voltage window 2.5-5V vs. Na^+/Na at a cycling rate of C/10 per Na^+.

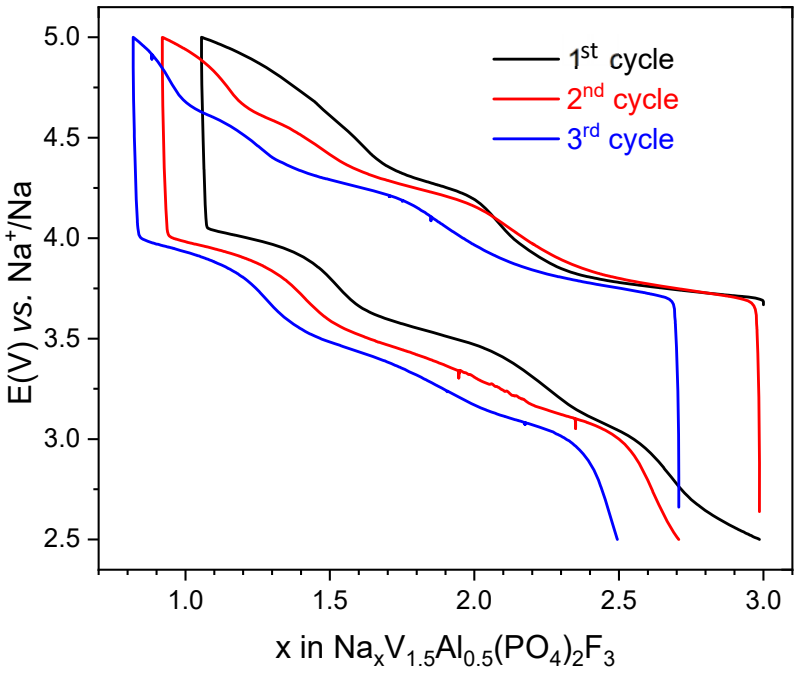

The extra-capacity accessible at high potential (> 4.5V) is not completely reversible and would come from electrolyte decomposition during cycling. Although the polarization increases during charge-discharge cycles when the voltage window is extended up to 5 V vs Na^+/Na, a sloping plateau can be observed at 4.65 V for the 2nd and 3rd charge. However, additional experiments such as operando X-ray absorption spectroscopy are needed in order to determine the origin of this sloping plateau.

1 M. Bianchini, N. Brisset, F. Fauth, F. Weill, E. Elkaim, E. Suard, C. Masquelier and L. Croguennec, *Chem. Mater.*, 2014, **26**, 4238–4247.

2 M. Bianchini, P. Xiao, Y. Wang and G. Ceder, *Adv. Energy Mater.*, 2017, **7**, 1700514.

3 L. H. B. Nguyen, T. Broux, P. S. Camacho, D. Denux, L. Bourgeois, S. Belin, A. Iadecola, F. Fauth, D. Carlier, J. Olchowka, C. Masquelier and L. Croguennec, *Energy Storage Mater.*, 2019, **20**, 324–334.

* Corresponding author (Laurence.Croguennec@icmcb.cnrs.fr)